Application of X-ray stress measurement for residual stress analysis by inherent strain method - Comparison of cos α and sin2 Ψ method-

メタデータ	言語: eng 出版者: 公開日: 2021-04-05 キーワード (Ja): キーワード (En): 作成者: メールアドレス: 所属:
URL	https://doi.org/10.24517/00061506

Bulletin of the JSME
Vol.4, No.5, 2017
Mechanical Engineering Journal

Application of X-ray stress measurement for residual stress analysis by inherent strain method - Comparison of cosα and sin$^2\psi$ method-

Mariko MATSUDA*, Keisuke OKITA**, Tomokazu NAKAGAWA** and Toshihiko SASAKI***
* Technical Development Department, Steel Casting & Forging Division, KOBE STEEL, LTD.
2-3-1 Shinhama Arai-cho, Takasago-shi, Hyogo 676-8670, Japan
E-mail: matsuda.mariko@kobelco.com
** Mechanical Engineering Laboratory, KOBE STEEL, LTD.
1-5-5 Takatsukadai, Nishi-ku, Kobe-shi, Hyogo 651-2271, Japan
*** Graduate School of Natural Science & Technology, Kanazawa University
Kakuma-machi, Kanazawa, 920-1192, Japan

Received: 12 January 2017; Revised: 14 April 2017; Accepted: 9 May 2017

Abstract
Most cold forming processes are perceived as simple surface treatments without a heating process and are widely used to improve the fatigue strength of various engineering components. The method for measuring the residual stresses caused by such surface treatment is very important when evaluating the fatigue strength of engineering components. The inherent strain method is one of the most effective measures for predicting the internal residual stress distribution. The residual stresses within a body are caused by internal permanent strains known as inherent strain or eigenstrain. In the case of cold formed components, the inherent strains are induced by plastic deformation. If a component is cut, the residual stress distribution changes, but the inherent strains of the original shape before cutting are preserved. The inherent strains are predicted by the inverse analysis of a finite element model using the measurement results of residual stresses on the slice or the cut surface of a body. On the other hand, a two-dimensional X-ray diffraction system based on a cosα method is useful for measuring the residual stresses because of its compactness and higher measurement speed than the conventional sin$^2\psi$ method. In this paper, we propose an efficient approach that combines the inherent strain method and an X-ray stress measurement along with a new measurement procedure for the fillet portion of an axisymmetric shaft with a flange after the cold forming process. This report compares the results estimated using the inherent strain method by the sin$^2\psi$ and cosα methods, and confirms that the differences in the results were very small. Furthermore, three advantages of the cosα method—wider measurable area, shorter measurement time, and shear stress measured at the same time as normal stress—are examined. Consequently, it is verified that the cosα method is effective for the proposed new approach.

Keywords : Residual stress, Inherent strain, Finite element method, X-ray stress measurement, cosα method, Cold forming process

1. Introduction

The development of high strength steels has recently been recognized to be reaching its upper strength limit. Therefore, most surface treatments, e.g., induction hardening, nitriding, shot peening, and cold rolling etc., are used to improve the fatigue strength of various engineering components. In particular, cold forming methods are applied as a simple method without a heating process. However, not only compressive residual stresses produced in the surface layer, but also tensile residual stresses are produced within it after surface treatments. To evaluate the fatigue strength of engineering components after surface treatments, the surface and internal residual stress distributions must be

Paper No.17-00022
J-STAGE Advance Publication date: 19 May, 2017
[DOI: 10.1299/mej.17-00022]

confirmed. Although there are many residual stress measurement techniques, techniques for the internal residual stress are limited to certain methods, e.g., neutron diffraction, the hole-drilling method, the inherent strain method, and so on. However, neutron diffraction needs special devices, and the hole-drilling method limits the measured position within a physical space. Consequently, the inherent strain method is one of the most effective methods for predicting the internal residual stress distribution of industrially produced components.

The residual stresses in an engineering component are caused by the internal permanent strains known as inherent strains or eigenstrains. If the component is cut, the residual stress distribution changes, but the inherent strains of the original shape before cutting are preserved. Therefore, the inherent strains are predicted by the inverse analysis of a finite element model using the measurement results of the released strains or residual stresses in the sliced or cut surface of an engineering component. Then, the residual stresses of the original shape can be analyzed using the predicted inherent strains. Recently, a two-dimensional X-ray diffraction system based on the $\cos\alpha$ method was developed and residual stresses can be measured more quickly than with the conventional $\sin^2\psi$ method. The $\sin^2\psi$ method requires X-ray diffraction data at several different incident angles; however, the residual stress can be calculated from one diffraction ring with a single incident angle using the $\cos\alpha$ method. Furthermore, the residual stresses in a narrow area can be measured by the $\cos\alpha$ method because the instrument of the $\cos\alpha$ method is more compact than the conventional $\sin^2\psi$ method. If X-ray $\cos\alpha$ measurements can be used for the inherent strain method, more data would be easily measured giving a higher estimated accuracy.

The general theory of the inherent strain method based on finite element analysis was proposed in the 1970s (Ueda, et al., 1975), and it was found that the inherent strain could be expressed as an appropriate function (Ueda and Ma, 1993). These methods have been shown to be effective for the estimation of the residual stresses in a welded joint in a reactor vessel (Nakacho, et al., 2009a, Nakacho, et al., 2014); however, the released strains of more than 2000 points were measured by strain gages in these studies. If a large number of residual stresses were measured, an X-ray diffraction system would be effective because the residual stresses could be measured more quickly than with other methods. The nondestructive evaluation of welding residual stresses based on inherent strain theory was proposed using X-ray diffraction for only the surface of a butt-welded plate (Ogawa, 2014). As X-ray diffraction can directly measure the residual strains, Korsunsky et al. proposed a framework for an inverse eigenstrain analysis to use the residual strains measured by synchrotron X-ray diffraction, and this method could be applied to a variety of surface treatment methods (Korsunsky, et al., 2006, Korsunsky, et al., 2007, Jun, et al., 2010, Jun, et al., 2011).

A two-dimensional X-ray diffraction system based on the $\cos\alpha$ method was proposed around the same period as the inherent strain method (Taira, et al., 1978). Subsequently, an imaging plate was developed as a two-dimensional X-ray detector (Miyahara, et al., 1986), and the entire diffraction ring could be obtained with high sensitivity and speed. Yoshioka et al. substantiated the possibility of measuring the stress using the Imaging Plate (IP) and $\cos\alpha$ method (Yoshioka, et al., 1990). Sasaki et al. established and proposed a system for X-ray stress measurement using the IP of a two-dimensional X-ray detector, which was the first worldwide (Sasaki and Hirose, 1995a). An X-ray stress measurement device using an IP suitable for the $\cos\alpha$ method was developed (Maruyama, et al., 2015). The possibility of triaxial stress analysis and the measurement of macro- and microstresses were investigated (Sasaki and Hirose, 1995b, Sasaki, et al., 1996), and it was confirmed that the oscillation method was effective for coarse-grained polycrystalline materials (Sasaki, et al., 1997). Further, a Fourier analysis could be applied for the determination of the stresses from the diffraction ring, (Miyazaki and Sasaki, 2014, 2015), and it is possible to determine the stresses using Fourier analysis with an imperfect diffraction ring (Fujimoto, et al., 2015).

In this study, we propose an efficient approach that combines the inherent strain method and X-ray stress measurements, and a new measurement procedure for the fillet portion of an axisymmetric shaft with a flange after the cold forming process. The prediction accuracy of this proposed method is verified by a comparison of the estimated results obtained from the X-ray $\cos\alpha$ and $\sin^2\psi$ methods. Moreover, the effectiveness of the X-ray $\cos\alpha$ measurement for the inherent strain method is confirmed.

2. Analytical method and measurement procedure

2.1 Specimen

An axisymmetric shaft with a flange, whose diameter is 500 mm, was prepared as shown in Fig. 1. The shaft is made of general low alloy steel that was quenched and tempered after forging. Table 1 lists the mechanical properties of the low alloy steel. A cold forming process was applied to the fillet portion between the shaft and the flange to

[DOI: 10.1299/mej.17-00022]

Table 1 Mechanical properties of the forged shaft made of general low alloy steel.

Tensile Strength (MPa)	0.2% Proof strength (MPa)	Elongation (%)	Reduction of Area (%)
902	750	18	63

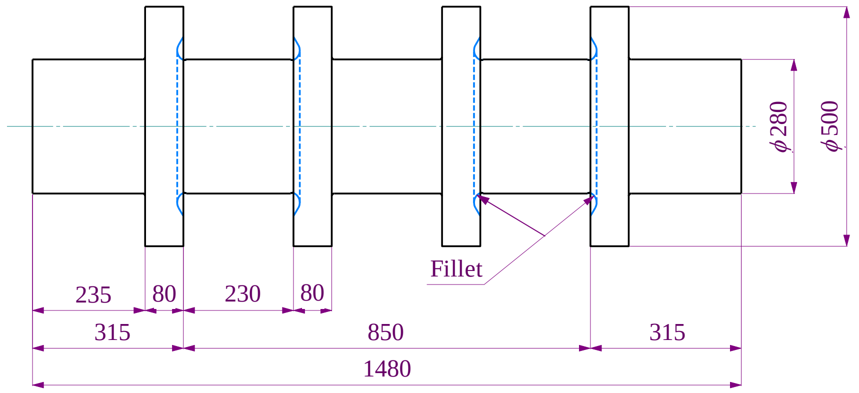

Fig. 1 Dimensions of the axisymmetric shaft with a flange.

improve the fatigue strength. Consequently, residual stresses were generated around the fillet, and the residual stress distribution was axisymmetric because the cold forming conditions were uniform in the circumferential direction.

2.2 Inherent strain method

We propose a new approach suitable for the fillet portion between the shaft and the flange for estimating the residual stress by the inherent strain method using X-ray stress measurement instead of measuring the released strains. The basic theory is as follows. The inherent strain distribution described with an appropriate function is useful for decreasing the number of unknowns determined by the proposed method. The relation between the inherent strain vector $\{\varepsilon_0\}$ and the inherent strain distribution coefficient vector $\{A\}$ can be expressed by the following elastic response equation:

$$\{\varepsilon_0\} = [\mathrm{P}]\{A\} \tag{1}$$

where [P] is the distribution function matrix.

The elastic strains due to the inherent strains exist in the surface-treated part of the body. This elastic strain vector $\{\varepsilon_K\}$ can be expressed as follows:

$$\{\varepsilon_K\} = [\mathrm{H}]\{A\} \tag{2}$$

where [H] is the elastic response matrix. The relation between the residual stresses and the elastic strain is defined by the elastic constitutive equation. The residual stress vector $\{\sigma_c\}$ can be expressed as follows:

$$\{\sigma_c\} = [\mathrm{M}]\{A\} \tag{3}$$

where [M] is the elastic response matrix. The [H] or [M] matrix can be obtained by repeating the following procedure. When one component of the vector $\{A\}$ is set to one and the other components of the vector $\{A\}$ are set to zero, the elastic strains or residual stresses are calculated by an FEM. Then when the next component of the vector $\{A\}$ is set to one and the other components of the vector $\{A\}$ are set to zero, the calculation by the FEM is conducted again.

The measured residual stresses do not completely correspond to the residual stresses calculated by Eq. (3) owing to measurement error. The differences between the measured and calculated residual stresses as the residuals are expressed as follows:

[DOI: 10.1299/mej.17-00022]

$$\{\nu_i\} = \{\sigma_{ci}\} - \{\sigma_{mi}\} \quad (i = 1 \cdots N) \tag{4}$$

where $\{\sigma_{ci}\}$ is the measured residual stress vector, $\{\sigma_{mi}\}$ is the calculated residual stress vector, and $\{\nu_i\}$ is the residual vector. The sum S of the squares of the residuals is calculated by the following equation:

$$S = \{\nu_i\}^T \{\nu_i\} \quad (i = 1 \cdots N) \tag{5}$$

The inherent strain distribution coefficient vector $\{A\}$ can be determined by the least-squares method to minimize S. In this study, as the shape of the specimen and the residual stress distribution are axisymmetric, two-dimensional finite element models are used, as shown in Fig. 2. Furthermore, the local cylindrical coordinate system at the center of the fillet, as shown in Fig. 3, is applied.

Nakacho et al. determined the applicability of two types of inherent strain distribution functions—multi-order and trigonometric functions—for a welded joint at the pipe penetration part of an actual reactor vessel (Nakacho, et al., 2009b). They selected the multi-order function as the more suitable one for their study. The difference in the results estimated by two functions, however, is very small according to their study and the suitable function may depend on the inherent strain distribution for different causes. We have already checked that the difference in the results estimated by the multi-order and trigonometric functions is very small, and the following function is suitable for a smooth inherent strain distribution caused by the cold-forming process. Consequently, the inherent strain distribution in this study is expressed as follows:

$$P(\xi,\omega) = \sum_{i=1}^{m}\sum_{j=1}^{n} A_{ij}(1-\xi)^i \sin(j\pi\omega) \tag{6}$$

$$\xi = \frac{R-R_0}{\Delta R}, \quad \omega = \frac{\alpha-\alpha_0}{\Delta\alpha} + \frac{1}{2} \tag{7}$$

where A_{ij} is the inherent strain distribution coefficient; m and n are the orders of the function (radial and tangential directions, respectively); R and α are the local cylindrical coordinates at the center of the fillet (radial and tangential directions, respectively); R_0 and α_0 are the reference points of the inherent strain region (radial and tangential directions, respectively); and ΔR and $\Delta\alpha$ are the increment values (radial and tangential directions, respectively). These parameters are shown in Fig. 3.

In the case of cold formed components, the inherent strains are induced by plastic deformation. The incompressibility of the plastically deformed metal is considered, and the inherent strains are set to zero on the boundary of the inherent strain region in Eq. (7) to determine the inherent strain distribution coefficient.

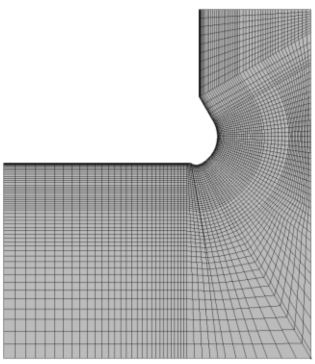

Fig. 2 Two-dimensional finite element model.

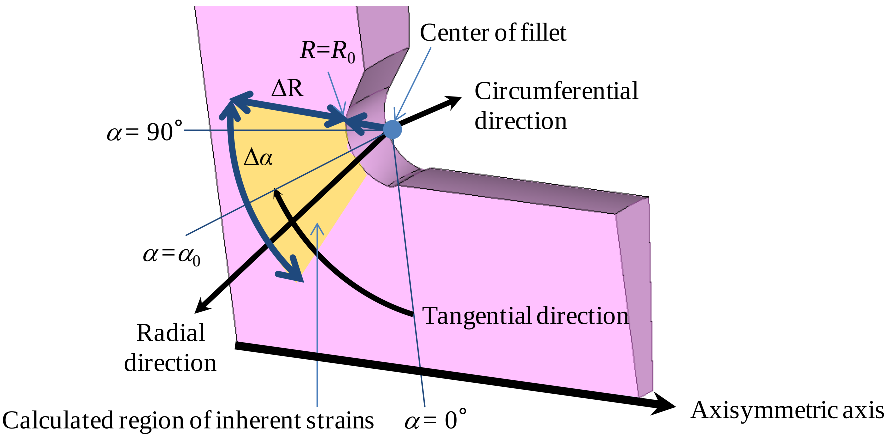

Fig. 3 Local cylindrical coordinates, the calculated region of inherent strains, and the dimensions of the axisymmetric shaft with a flange.

2.3 Residual stress measurement by the X-ray diffraction technique

To evaluate the fatigue strength of the fillet portion of the axisymmetric shaft with a flange, it is necessary to confirm the residual stresses in the local cylindrical coordinate system defined at the center of the fillet, as shown in Fig.3. The fillet angle α is defined in the tangential direction and the fillet angle of 0° is defined at the position where the tangential direction is vertical to the axisymmetric axis.

The measured positions can be chosen freely in the theory of the inherent strain method. In actuality, however, the accuracy of the estimated results at a position without the measured points would be worse because of the effect of the measurement error. The measured positions should be set to the position at which the residual stresses are wanted for use in the fatigue analysis. Therefore, we propose a new measurement procedure for the fillet portion when using the inherent strain method, as shown in Fig. 4. The conventional method uses T specimens sliced in the transverse direction and L specimens sliced in longitudinal directions. In this study, T specimens were used, and cone-shaped (C) specimens, whose surfaces were machined along different fillet angles, were used instead of L specimens. Figure 5 shows an example of the stress distribution of the fillet portion and a comparison between the L and C specimen cutting lines. If L specimens were applied, the steep gradient distribution of the residual stresses could not be measured because many measurement positions could not be set on the surface of the fillet. The residual stresses in the fillet surface of the original shape could not be measured by the X-ray diffraction system because of a lack of sufficient

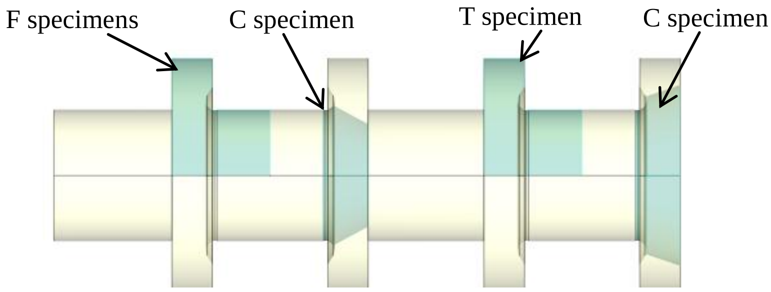

(a) Sampling positions of the T, C, and F specimens.

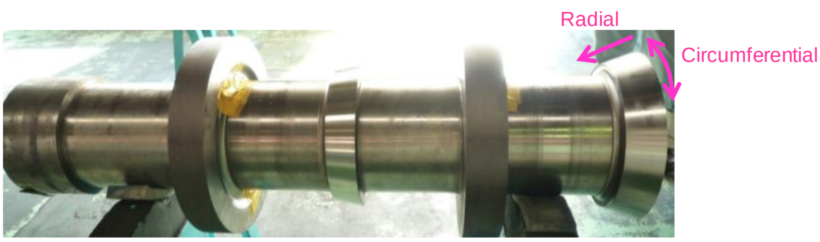

(b) Example of the actual shape of a C specimen.

(c) Actual shape of a T specimen.

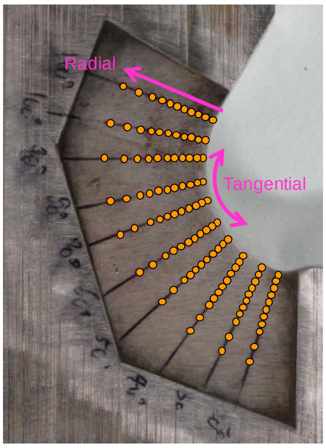

(d) Measurement positions on the surface of a T specimen.

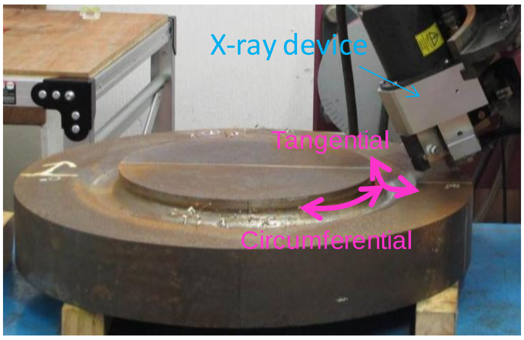

(e) Measurement state of the X-ray $\sin^2\psi$ method on the fillet of the F specimen.

Fig. 4 Sampling position, actual shape, measurement positions, and state of a new measurement procedure for the fillet portion of an axisymmetric shaft with a flange.

[DOI: 10.1299/mej.17-00022]

Table 2 Conditions and the number of points for the X-ray measurement.

	$\sin^2\psi$ method	$\cos\alpha$ method
Equipment	Rigaku : MSF-3M	Pulstec : μ-X360
Characteristic X-ray	Cr-Ka	
Diffraction plane	α-Fe (211)	
Tube voltage	30 kV	
Tube current	10.0 mA	1.0 mA
Irradiated area	3 × 3 mm^2, rectangle	2 mmφ
Fixed time	1 s	30 s
ψ_0 tilt angle	0, 10, 18, 24, 30, 35, 40°	35°
The number of points on T specimen	222	232
The number of points on C specimen	308	
The number of points on F specimen	28	

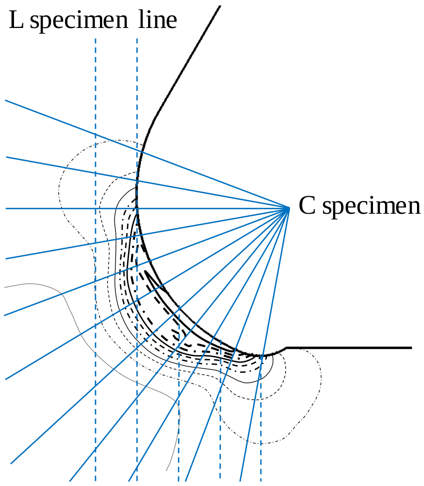

Fig. 5 Example of the stress distribution of the fillet portion and a comparison of the L and C specimen cutting lines.

space for the X-ray apparatus. Therefore, a flange section cut from the shaft (F specimen) was also used. However, the residual stresses in the tangential direction at the positions of the fillet near the shaft (fillet angle < 70°) could not be measured using the X-ray $\sin^2\psi$ method on the same reason stated above. Then, the residual stresses in the surfaces of all specimens were measured using the X-ray $\sin^2\psi$ method. Further, the residual stresses of only the T specimen at the same point were measured by both the X-ray $\cos\alpha$ and $\sin^2\psi$ methods to compare the results. If all specimens were measured by both methods, a considerable cost and time would be required.

Electropolishing to a depth of 0.2-0.3mm, where the depth depends on the condition of the specimens, was carried out to eliminate the effects of cutting, rust, etc. The position changes by electropolishing were considered in an inverse analysis, and all values of the residual stress were corrected by the SAE method (SAE J784a, 1971). The measurement positions on the T specimen are shown in Fig. 4 (d). The residual stresses in the T specimen were measured along with the fillet angle from 0° to 110° in intervals of 10° and in depth direction along the fillet radius until 18 or 40 mm. The residual stresses in the C specimen were measured along with the fillet angle from 20° to 110° in intervals of 10° and at the same position and in the same depth direction along the fillet radius as the T specimen. In the case of the F specimen, the measurable fillet angle for a sufficient intensity of X-rays was limited to 80° or larger because $\sin^2\psi$ method needs to acquire X-ray diffraction data at the several different incident angles. Therefore, electropolishing was additionally carried out to measure the residual stresses of the F specimen at a depth of 0.5 mm from the surface to increase the number of measurement points. If a compact instrument based on the $\cos\alpha$ method was applied, the residual stresses in the surface of the F specimen for all fillet angles could be measured. In this study, however, the residual stresses of only the T specimen were measured by the $\cos\alpha$ methods. Then, the residual stresses in the

[DOI: 10.1299/mej.17-00022]

tangential direction for all fillet angles on the surface of only the T specimen were measured by the X-ray cosα method. The conditions and the number of points for the X-ray measurement are listed in Table 2.

2.4 Residual stress measurement by the drilling method

To verify the accuracy of results analyzed by the inherent strain method, the internal residual stresses along the direction at a fillet angle of 40° were measured by a hole-drilling method. The results measured by the hole-drilling method would be affected by the drilling process; however, this method is acknowledged as one of the applicable industrial methods for obtaining reasonable values for the inner residual stresses. In this study, the values measured by the hole-drilling method are applied as a criterion for the accuracy of the results estimated by the inherent strain method. The measurement procedure of the hole-drilling method is shown in Fig. 6. Holes with different depths were drilled into the fillet of the original shape of the specimen along the circumferential direction because the specimen was antisymmetric in this study. Then, strain gauges were attached to the bottoms of the holes, and vicinity surrounding each strain gauge was cut into minimum sized pieces to release the residual strains. Finally, the released strains were measured and converted into the residual stresses.

3. Evaluation of the estimated residual stresses

3.1 Measurement results for the cut specimens

Figure 7 shows a comparison of the residual stresses in the surface of the T specimen measured by the X-ray cosα and sin$^2\psi$ methods at fillet angles of 30° and 40°. There are slight differences in the values obtained by the two methods, but the same tendency in the distribution of the residual stresses is confirmed. Some data measured by the cosα method have a larger standard deviation than those of the sin$^2\psi$ method. This is because the sin$^2\psi$ method needs X-ray diffraction data at several different incident angles, whereas the cosα method needs X-ray diffraction data at only one incident angle. Some data with a larger standard deviation measured by the cosα method tend to differ more from the results of the sin$^2\psi$ method. In addition, the slight differences in both X-ray measurements might be caused by the slight differences in the measurement positions and measurement errors.

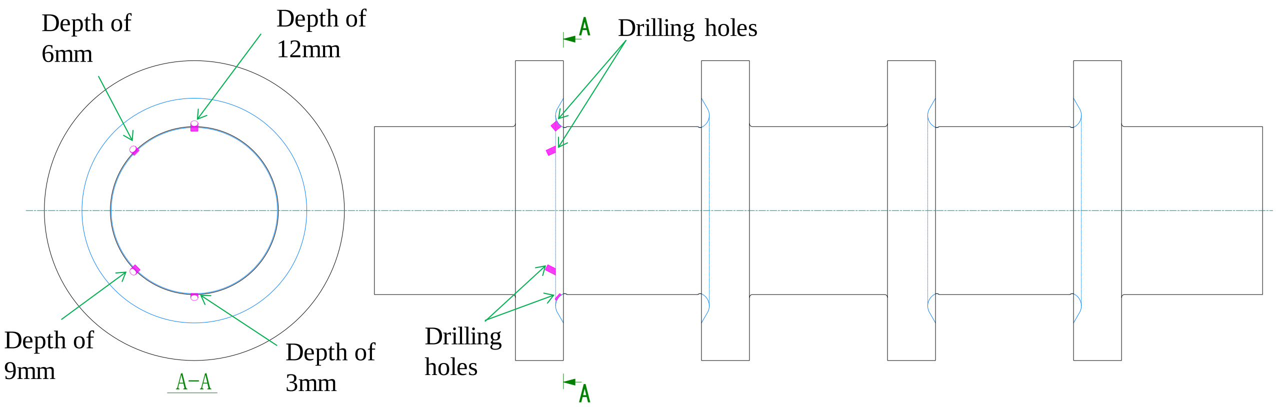

(a) Positions of the drilling holes on the fillet portion.

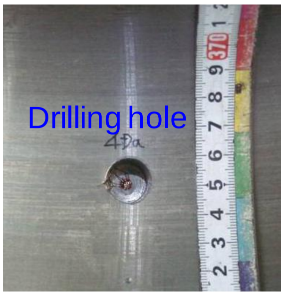

(b) Example of an actual drilling hole and strain gauge.

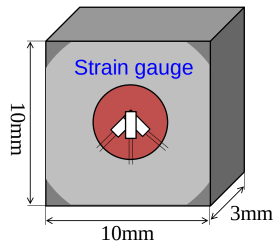

(c) Size of the minimum pieces.

Fig. 6 Measurement procedure of the hole-drilling method.

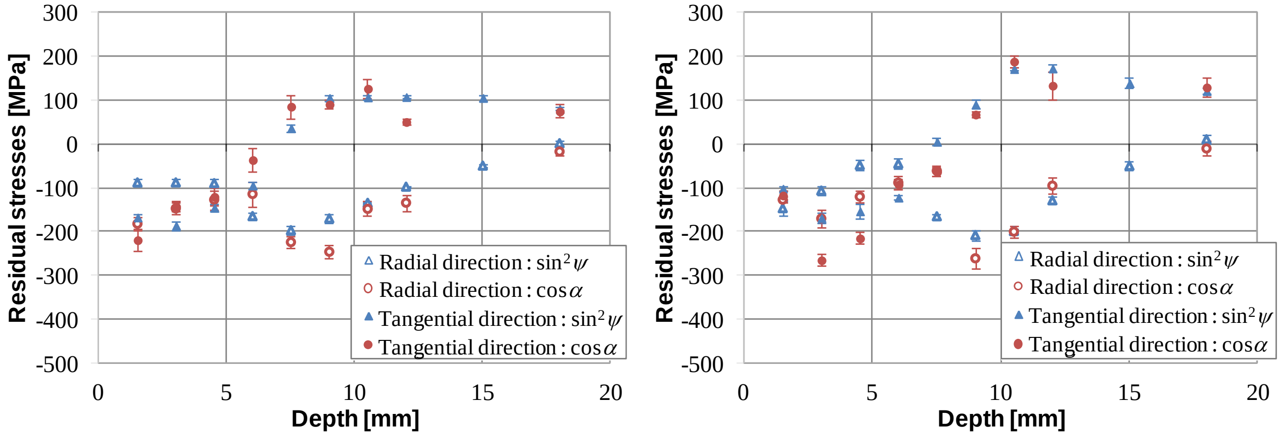

(a) 30° fillet angle

(b) 40° fillet angle

Fig. 7 Comparison of the residual stress measurements obtained by the X-ray $\cos\alpha$ and $\sin^2\psi$ methods on the surface of the T specimen along directions at fillet angles of 30° and 40°.

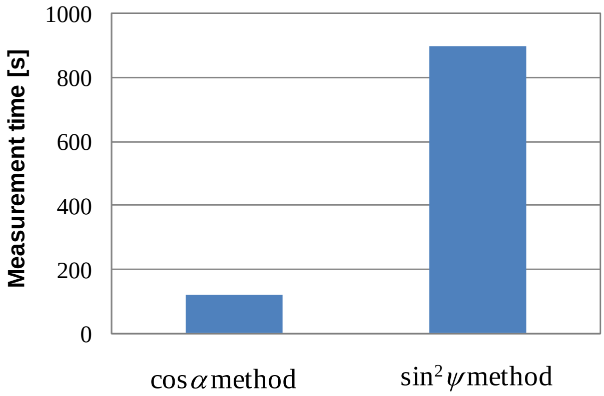

Fig. 8 Comparison of the measurement times per one point for the $\cos\alpha$ and $\sin^2\psi$ methods.

The present work used over 558 data points measured by the X-ray stress measurement; therefore, a considerable amount of time was required. Figure 8 shows a comparison of the measurement times per one point for the $\cos\alpha$ and $\sin^2\psi$ methods. It is confirmed that the $\cos\alpha$ method is almost seven times faster than the $\sin^2\psi$ method in real operating time.

3.2 Effect of the order of the inherent strain distribution function

It is important to determine the number of coefficients in the inherent strain distribution function. The effects of the number of coefficients on the accuracy of the results estimated by the inherent strain method were examined. The inherent strain distribution coefficient vectors could be determined by the least-squares method to minimize the sum of the squares of the differences between the measured and estimated residual stresses. The root mean square error (RMSE) of these differences is used as an evaluation index to investigate the accuracy of the estimated results. Table 3 summarizes the regional parameters in the inherent strain method, and Fig. 9 shows RMSE versus the number of coefficients of the inherent strain distribution function in each stress component (m times n). The RMSE tends to be linearly dependent upon the total number of coefficients with a negative slope.

In this study, it is thought that the estimated results of the inherent strain method should correspond to the measurement values by the hole-drilling method from an industrial viewpoint. The influence of the order of the coefficients in the inherent strain distribution function on the estimated results was investigated. Figure 10 shows a comparison between the estimated results using the residual stresses measured by the $\sin^2\psi$ method and the measurements with the hole-drilling method at a fillet angle of 40°. It is confirmed that extremely large compressive stresses in the tangential direction are estimated at the surface when m is 4 and n is 6. The reason for the occurrence of this phenomenon is that there are no measured data in the tangential direction at the surface and the estimated results can be

[DOI: 10.1299/mej.17-00022]

significantly changed to minimize the sum of the squares of all of the differences between the measured and estimated results by the least-squares method with the total order of the coefficients in the inherent strain distribution function. In contrast, when m is 2, the above phenomenon does not occur because the shape of the inherent strain distribution in the radial direction is limited. When m is 2 and n is greater than 15, the estimated stresses in the circumferential direction greatly differ from the measurement data. When the order of the coefficients in the inherent strain distribution function is set to a value that is too large, the estimated results are more easily affected by the measurement error. This means that a suitable order of the coefficients in the inherent strain distribution depends on the number of measurements and the position.

3.3 Comparison between the cosα and sin$^2\psi$ methods

Figure 11 shows the differences of the estimated results using the residual stresses measured by the X-ray cosα and sin$^2\psi$ methods and the comparison between the estimated results and the measurements via the hole-drilling method at a fillet angle of 40° when m is 3 and n is 6. The results estimated using the X-ray cosα method substantially correspond

Table 3 Regional parameters in the inherent strain method.

Regional parameter in the radial direction R_0 [mm]	21.5
Regional parameter in the radial direction ΔR [mm]	13.0
Regional parameter in the circumferential direction α_0 [°]	50
Regional parameter in the circumferential direction $\Delta\alpha$ [°]	140

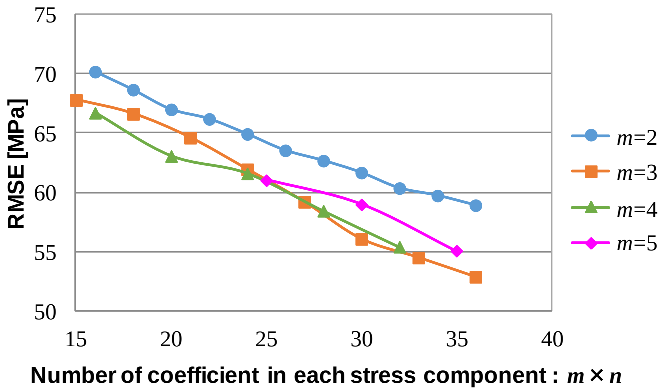

Fig. 9 RMSE of the differences between the measured and estimated residual stresses versus the number of coefficients of the inherent strain distribution function in each stress component (m times n).

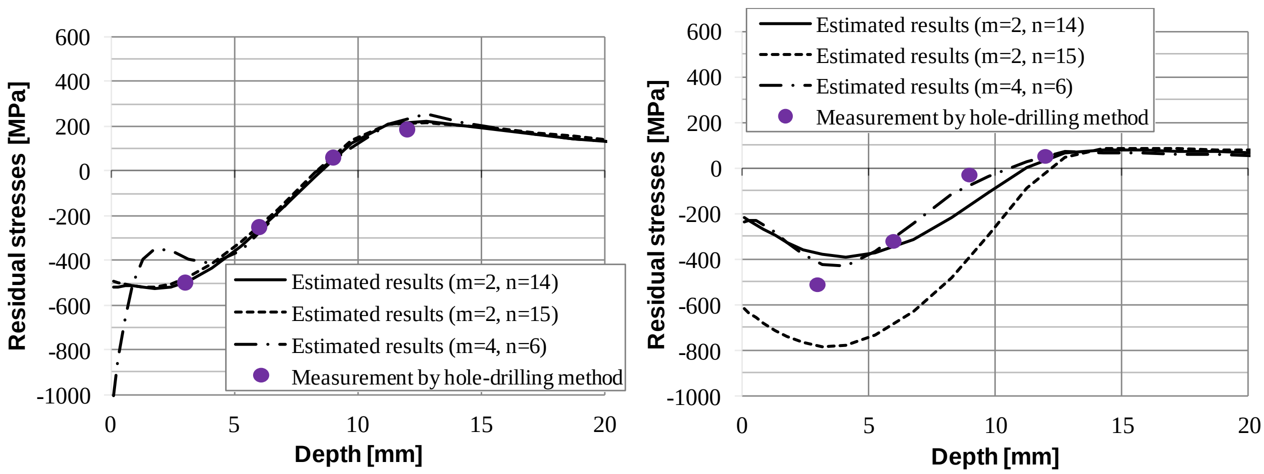

(a) Tangential direction (b) Circumferential direction

Fig. 10 Comparison between the estimated results using the residual stresses measured by the sin$^2\psi$ method and the measurements with the hole-drilling method at a fillet angle of 40°.

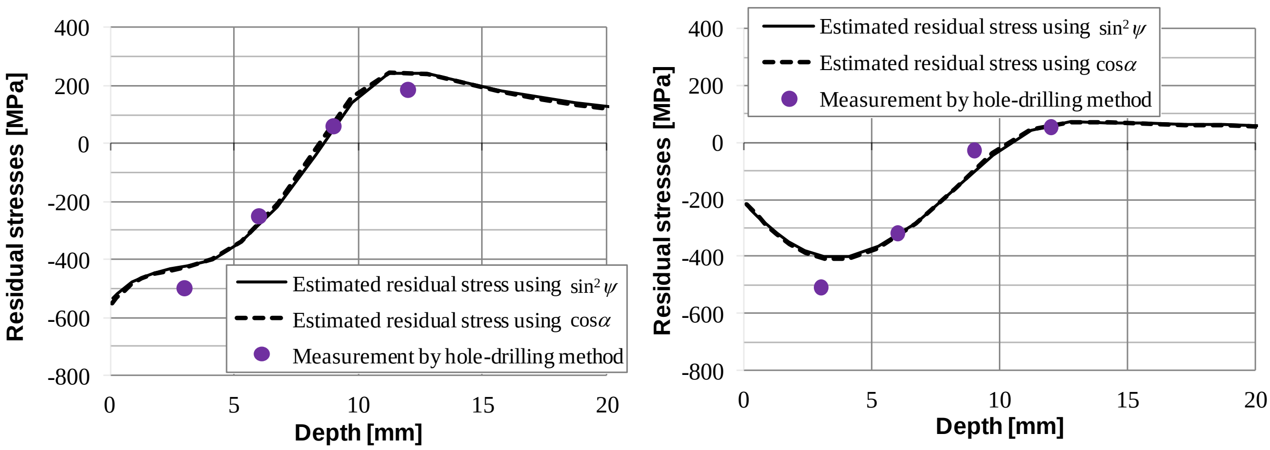

(a) Tangential direction (b) Circumferential direction

Fig. 11 Differences of the estimated results using the residual stresses measured by the X-ray cosα and sin$^2\psi$ methods and the comparison between the estimated results and the measurements via the hole-drilling method at a fillet angle of 40° when *m* is 3 and *n* is 6.

with those using the sin$^2\psi$ method. A large measurement error might affect the estimated results in the inherent strain method generally, however in this study, the difference of the values measured by cosα and sin$^2\psi$ methods hardly affected the results because the difference was very small and both distributions of the residual stresses were same tendency, as shown in Fig. 7. It follows from Fig. 10 and Fig. 11 that the order of the function of the inherent strain distribution affects the estimated results more sensitively than the slight differences between the values obtained by the X-ray cosα and sin$^2\psi$ methods. It is verified that the X-ray cosα technique can be applied to the inherent strain method in the same way as the sin$^2\psi$ method.

3.4 Efficiency of the X-ray cosα technique

The final objective of this study is to confirm the efficiency of the X-ray cosα method for the inherent strain method. There are three advantages of the application of the X-ray cosα method to the inherent strain method. The first is that the measurable area of the cosα method in the tangential direction is wider than that in the sin$^2\psi$ method. The second is that the measurement time of the cosα method is lower than that of the sin$^2\psi$ method, and the third is that the shear stresses can be analyzed at the same time as the normal stresses by the cosα technique from the full diffraction ring using an IP. These advantages are examined in more detail.

First, the effect of the wider measurable area of the residual stresses is discussed. The residual stresses in the tangential direction on the surface of the fillet could be measured by the sin$^2\psi$ method only at the fillet angle greater than 80° for a sufficient intensity of X-rays. The sin$^2\psi$ method needs a much wider space for measurement than the cosα method because the sin$^2\psi$ method requires X-ray diffraction data at several different incident angles. If a compact X-ray instrument based on the cosα method was used for the F specimen, the residual stresses in the tangential direction could be measured for the entire range of fillet angles. In this study, however, the residual stresses of only the T specimen were measured by the cosα methods. Figure 12 shows a comparison of the estimated results with and without the surface data of the T specimen in the tangential direction. The same tendency as that in Fig. 10 is confirmed without the surface data. However, the estimated results for the surface of the specimen are not significantly changed, and the accuracy in the circumferential direction is improved with the surface data of the T specimen when *m* is 4 and *n* is 10. It is important to mention here that a larger order of the coefficients in the inherent strain distribution function than that in the sin$^2\psi$ method can be used, and the accuracy of the estimated results can be improved if the residual stresses in the tangential direction can be measured over the wider surface of the specimen.

Next, the influence of the shorter measurement time is examined. It is proposed that the number of measurement results depends on the measurement time because the costs of measurement might be limited in an industrial setting. Figure 13 shows a comparison of the estimated results using all of the data and half of the data. The residual stresses in the circumferential direction of the specimen were measured at a pitch of 10° in this study. For half of the data, the measurement results at the even angles in the circumferential direction at a pitch of 20° were used. When the number of the measurement results in the circumferential direction is decreased, it is necessary to decrease the order of the

[DOI: 10.1299/mej.17-00022]

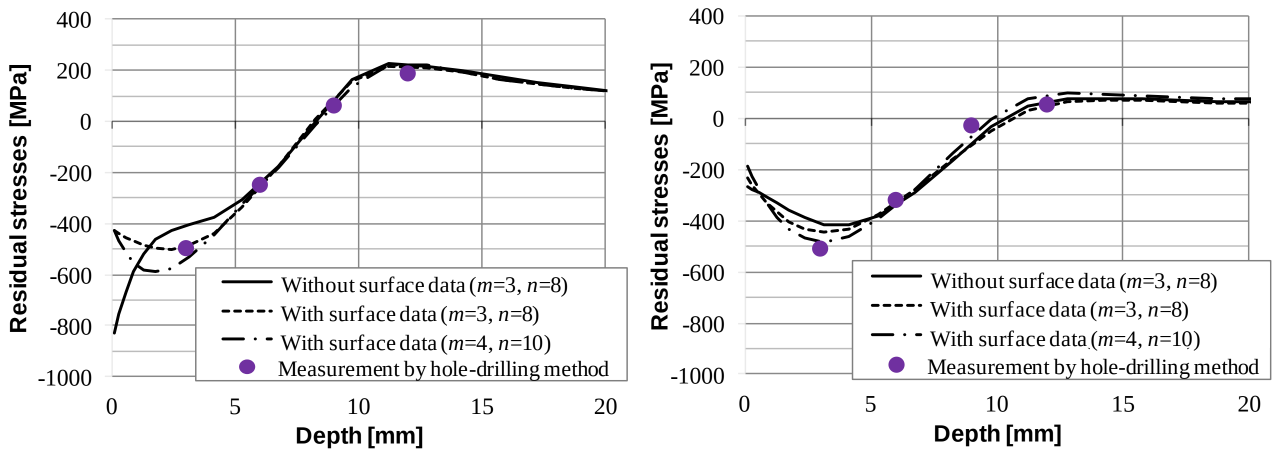

(a) Tangential direction (b) Circumferential direction

Fig. 12 Influence of the use of surface data in tangential direction for the surface of the T specimen on the differences between the estimated results and the measurements via the hole-drilling method at a fillet angle of 40°.

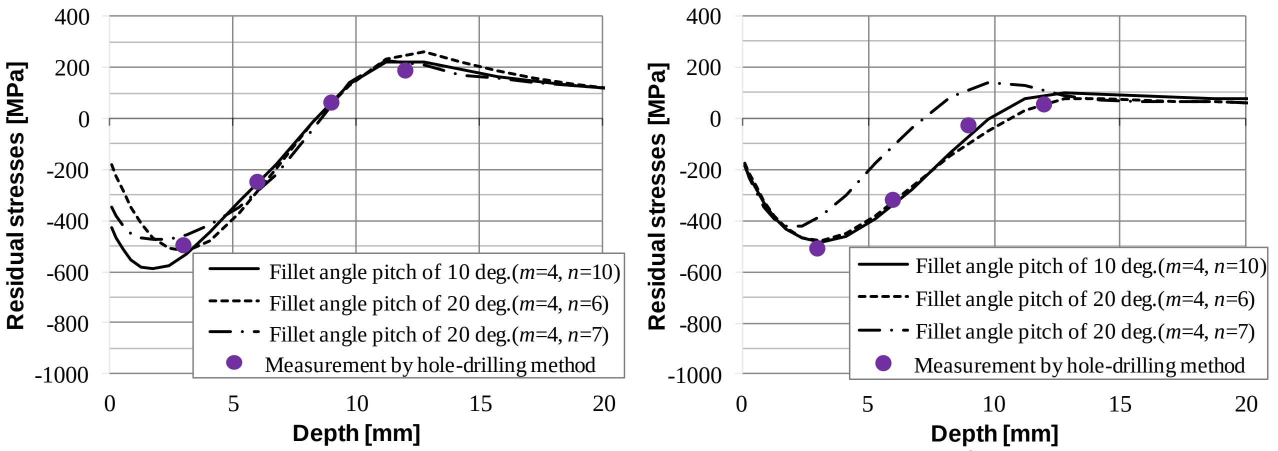

(a) Tangential direction (b) Circumferential direction

Fig. 13 Influence of the reduction in the number of measurement points in circumferential direction on the differences between the estimated results and the measurements via the hole-drilling method at a fillet angle of 40°.

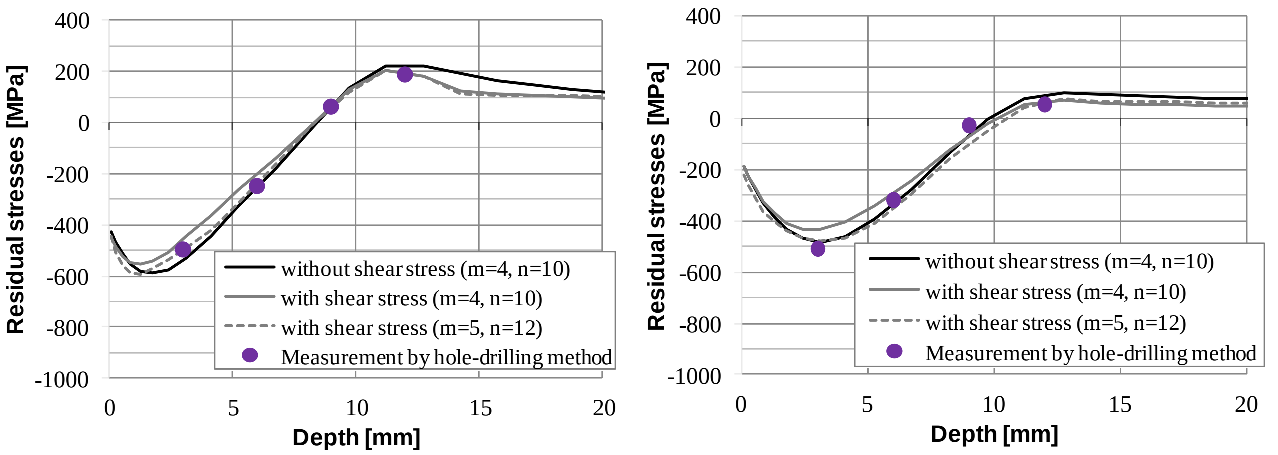

(a) Tangential direction (b) Circumferential direction

Fig. 14 Influence of the use of shear stresses for the surface of the T specimen on the differences between the estimated results and the measurements via the hole-drilling method at a fillet angle of 40°.

inherent strain distribution function, resulting in a decrease in the estimated accuracy. Conversely, if a larger number of results were measured by the cosα method at realistic costs, the accuracy could be further improved. The residual stresses around the generation region of the inherent strain can be mapped using the cosα measurement in an industrial setting, resulting in a high accuracy for the results estimated by the inherent strain method.

Finally, the effect of the use of shear stress is examined. Figure 14 shows a comparison of the estimated results when using and not using shear stress. The results estimated when not using shear stress have a higher accuracy than those using shear stress when the same order of the inherent strain distribution function is applied. If a larger order of the inherent strain distribution function is applied, the accuracy of the estimated results using shear stresses will be slightly improved, but the large difference cannot be confirmed for the results with and without shear stress. It is considered that the effect of using shear stresses cannot be confirmed because shear residual stresses are smaller than the normal residual stresses in this study. If the accuracy of the measured shear stresses became higher than that presented here, the accuracy of the estimated results might be improved.

4. Conclusion

A new approach that combines the inherent strain method, X-ray measurements, and a new measurement procedure for the fillet portion of an axisymmetric shaft with a flange after a cold forming process was proposed. It is confirmed that the suitable order of the coefficient of the inherent strain distribution function depends on the number of measurement data points and the position, and the accuracy of the estimated results is greatly decreased when the order of the coefficients of the inherent strain distribution function is greater than the suitable one. Furthermore, it is verified that the X-ray cosα method can be applied to the inherent strain method in the same way as the $\sin^2\psi$ method because the order of the function of the inherent strain distribution affects the estimated results more sensitively than the slight differences in the values obtained by the X-ray cosα and $\sin^2\psi$ methods.

We consider there are three advantages to the application of the X-ray cosα measurement to the inherent strain method. A larger order of the coefficients of the inherent strain distribution function can be used when the residual stresses in a wider surface of the specimen are measured using a compact instrument based on the cosα method, resulting in a higher accuracy of the estimated results. Further, it is suggested that the accuracy will be further improved, if a larger number of results are measured by the cosα method because of the low measurement time. However, the effect of measuring the shear stresses at the same time as the normal stresses cannot be confirmed because the residual shear stresses are less than the normal residual stresses in this study. If the accuracy of the measured shear stresses became higher than those in the present study, the accuracy of the estimated results could be improved.

It follows from these arguments that our proposed approach is efficient for evaluating the internal residual stresses in the fillet portion of an axisymmetric shaft with a flange after a cold forming process, and the X-ray cosα measurement is effective for improving the accuracy of the results estimated by the inherent strain method in this study.

References

Fujimoto, Y., Miyazaki, T., and Sasaki, T., X-ray stress measurement of ferritic steel using Fourier analysis of Debye-Scherrer ring, Journal of the Society of Materials Science, Vol. 64, No.7 (2015), pp.567–572 (in Japanese).

Jun, T.–S., and Koursunsky, A. M., Evaluation of residual stresses and strains using the eigenstrain reconstruction method, International Journal of Solids and Structures, Vol.47, No.13 (2010), pp.1678–1686.

Jun, T.–S., Venter, A. M., and Koursunsky, A. M., Inverse eigenstrain analysis of the effect of non-uniform sample shape on the residual stress due to shot peening, Experimental Mechanics, Vol.51, No.2 (2011), pp.165–174.

Korsunsky, A. M., Kim, K., Golshan, M., and Regino, G. M., Residual stress analysis in shot peened and fretting fatigued samples by the eigenstrain method, Materials Science Forum, Vol.524–525, (2006), pp.343–348.

Korsunsky, A. M., Regino, G. M., Latham, D. P., Li, H. Y., and Walsh, M. J., Residual stresses in rolled and machined nickel alloy plates: synchrotron X-ray diffraction measurement and three-dimensional eigenstrain analysis, The Journal of Strain Analysis for Engineering Design, Vol.42, No.1 (2007), pp.1–12.

Maruyama, Y., Miyazaki, T., and Sasaki, T., Development and validation of an X-ray stress measurement device using an image plate suitable for the cosα method, Journal of the Society of Materials Science, Vol.64, No.7 (2015), pp.560–566 (in Japanese).

Miyahara, J., Takahashi, K., Amemiya, Y., Kamiya, N., and Satow, Y., A new type of X-ray area detector utilizing laser stimulated luminescence, Nuclear Instruments and Methods in Physics Research Section A, Vol.246, No.1–3 (1986), pp.572–578.

Miyazaki, T., and Sasaki, T., X-ray stress measurement with two-dimensional detector based on Fourier analysis, International Journal of Materials Research, Vol. 105, No.9 (2014), pp.922–927.

Miyazaki, T., and Sasaki, T., Linearized analysis of X-ray stress measurement using the Debye-Scherrer ring, International Journal of Materials Research, Vol. 106, No.9 (2015), pp.1002–1004.

Nakacho, K., Ohta, T., Ogawa, N., Yoda, S., Sogabe, M., and Ogawa, K., Measurement of welding residual stresses by inherent strain method – New theory for axial-symmetry and application for pipe joint, Quarterly Journal of the Japan Welding Society, Vol.27, No.1 (2009a), pp.104–113 (in Japanese).

Nakacho, K., Ogawa, N., and Ohta, T., Measurement of welding residual stresses of reactor vessel by inherent strain method – Diagnosis of inherent strain distribution function, Quarterly Journal of the Japan Welding Society, Vol.27, No.4 (2009b), pp.297–306 (in Japanese).

Nakacho, K., Ogawa, N., Ohta, T., and Nayama, M., Inherent-strain-based theory of measurement of three-dimensional residual stress distribution and its application to a welded joint in a reactor vessel, Transactions of the ASME, Journal of Pressure Vessel Technology, Vol.136, No.3 (2014), p. 031401.

Ogawa, M., Non-destructive evaluation of welding residual stresses in the thickness direction via X-ray diffraction, Transactions of the Japan Society of Mechanical Engineers, Vol.80, No.815 (2014), p.SMM0195 (in Japanese).

Residual Stress Measurement by X-ray Diffraction - SAE J784a, Report of Iron and Steel Technical Committee Approved September 1960 and Last Revised by Fatigue Design and Evaluation Committee August 1971, (1971), pp.62–65, Society of Automotive Engineers, Inc.

Sasaki, T., and Hirose, Y., Single incidence X-ray stress measurement for all plane stress components using imaging plate of two-dimensional X-ray detector, Journal of the Society of Materials Science, Vol.44, No.504 (1995a), pp.1138–1143 (in Japanese).

Sasaki, T., and Hirose, Y., X-ray triaxial stress analysis using whole diffraction ring detector with imaging plate, Transactions of the Japan Society of Mechanical Engineers, Series A, Vol.61, No.590 (1995b), pp.2288–2295 (in Japanese).

Sasaki, T., Lin, Z., and Hirose, Y., X-ray measurement of macro- and microstresses using imaging plate and its application to ferritic and austenitic dualphase stainless steel, Transactions of the Japan Society of Mechanical Engineers, Series A, Vol. 62, No.604 (1996), pp.2741–2749 (in Japanese).

Sasaki, T., Hirose, Y., and Yasukawa, S., X-ray stress measurement of coarse-grained polycrystalline materials by imaging plate method, Transactions of the Japan Society of Mechanical Engineers, Series A, Vol. 63, No.607 (1997), pp.533–541 (in Japanese).

Taira, S., Tanaka, K., and Yamasaki, T., A method of X-ray microbeam measurement of local stress and its application to fatigue crack growth problems, Journal of the Society of Materials Science, Vol.27, No.294 (1978), pp.251–256 (in Japanese).

Ueda, Y., Fukuda, K., Nakacho, K., and Endo, S., A new measuring method of residual stresses with the aid of finite element method and reliability of estimated values, Journal of the Society of Naval Architects of Japan, Vol.138, (1975), pp.499–507 (in Japanese).

Ueda, Y., and Ma, N.X., Expression of inherent strain in form of function and its estimation: Estimating and measuring methods of residual stresses using inherent strain distribution described as functions (Report 1), Quarterly Journal of the Japan Welding Society, Vol.11, No.1 (1993), pp.189–195 (in Japanese).

Yoshioka, Y., Ohya, S. and Shinkai, T., Application of imaging plate to micro-beam X-ray diffraction, Journal of the Japanese Society for Non-Destructive Inspection, Vol.39, No.8 (1990), pp.666–671 (in Japanese).

[DOI: 10.1299/mej.17-00022]